

246.2 K, ~11 Torr for *n*-propyl nitrite at 240.6 K, and <3 Torr for *n*-butyl nitrite at 240.6 K.

Two further checks can be made on the ability of RRKM theory to model the experimental rate constants. First, k_{∞} values calculated by the model should agree reasonably well with the experimental values. Infinite-pressure rate constants were calculated from eq 14. The calculated k_{∞} values for the syn \rightarrow anti reaction

$$k_{\infty} = \left[\frac{L^{\ddagger} Q_1^{\ddagger}}{h Q_1 Q_2} e^{-E_0/RT} \Delta E \right] \left[\sum_{i=1}^{i_{\max}} \sum_{\rho} \rho(E_i^{\ddagger}) e^{-E_i^{\ddagger}/RT} \right] \quad (14)$$

are as follows: methyl, 381 s⁻¹; ethyl, 586 s⁻¹; *n*-propyl, 232 s⁻¹; and *n*-butyl, 202 s⁻¹. These are in satisfactory agreement with the experimental values calculated from eq 4: methyl, 360 s⁻¹; ethyl 555 s⁻¹; *n*-propyl, 205 s⁻¹; and *n*-butyl, 165 s⁻¹. Second, the value of ω at the experimental $P_{1/2}$ is equal to the rate of deactivating collisions. Assuming correctness of the Lindemann mechanism, this value must equal the calculated value of $\langle k(E^*) \rangle$, the average rate that energized molecules become products. Table

II lists these values which are in good agreement for all four nitrites.

Agreement between theoretical pseudounimolecular, specific, and infinite-pressure rate constants calculated from reasonable values of vibrational frequencies, collision diameters, collision efficiencies, and threshold energies using RRKM kinetic theory and the values obtained from the falloff of the experimental rate constants obtained from NMR line-shape analysis of exchange region DNMR spectra give strong support to the conclusion that internal vibrational energy redistribution in this homologous series of alkyl nitrites is rapid, compared to $\langle k(E^*) \rangle$, and statistical. This indicates that the increased number of vibrational states due to each additional methylene group may participate in the IVR process, and energy acquired in these states is available for the conformational exchange process in all the nitrites studied.

Acknowledgment. We are pleased to acknowledge the National Science Foundation (CHE 85-03074 and CHE 83-50 1698 (PYI)), the National Institute of Health (GM 29984-04), and the Alfred P. Sloan Foundation for the support of this research.

Kinetics of the Reactions of HS and HSO with O₃

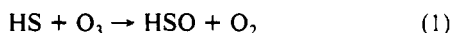
Niann S. Wang and Carleton J. Howard*

Aeronomy Laboratory, National Oceanic and Atmospheric Administration, 325 Broadway, Boulder, Colorado 80303, and the Department of Chemistry and Biochemistry and the Cooperative Institute for Research in Environmental Sciences, University of Colorado, Boulder, Colorado (Received: January 10, 1990; In Final Form: June 18, 1990)

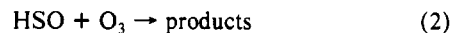
The kinetics of the reactions of HS and HSO with O₃ have been studied in a discharge flow system coupled to a laser magnetic resonance spectrometer: HS + O₃ \rightarrow HSO + O₂ (1); HSO + O₃ \rightarrow products (2). Measurements were made at low pressures (1–2.2 Torr) and temperatures between 296 and 431 K. The Arrhenius equation for reaction 1 is $k_1 = (1.1 \pm 0.2) \times 10^{-11} \exp((-280 \pm 50)/T) \text{ cm}^3 \text{ molecule}^{-1} \text{ s}^{-1}$. Our result for k_1 at room temperature is somewhat higher than the results of two previous studies. Reaction 2 has more than one channel: HSO + O₃ \rightarrow HS + 2O₂ (2a), which regenerates HS, and one or more competing processes that oxidize HSO further: HSO + O₃ \rightarrow products (2 α). The complex reaction mechanism required computer simulations to obtain: $k_{2a} = (7.0 \pm 2.0) \times 10^{-14}$ at 297 K, $(9.0 \pm 3.0) \times 10^{-14}$ at 377 K, and $(1.0 \pm 0.3) \times 10^{-13} \text{ cm}^3 \text{ molecule}^{-1} \text{ s}^{-1}$ at 404 K. The room-temperature k_{2a} value is in reasonable agreement with an earlier study. $k_{2\alpha}$ was measured directly to be $(3.5 \pm 1.5) \times 10^{-14} \text{ cm}^3 \text{ molecule}^{-1} \text{ s}^{-1}$ at 296 K and $(8.6 \pm 3.5) \times 10^{-14} \text{ cm}^3 \text{ molecule}^{-1} \text{ s}^{-1}$ at 404 K. The deuterium isotope effect on reactions 1 and 2a was also investigated, $k(\text{DS} + \text{O}_3 \rightarrow \text{DSO} + \text{O}_2) = (4.0 \pm 0.8) \times 10^{-12} \text{ cm}^3 \text{ molecule}^{-1} \text{ s}^{-1}$ and $k(\text{DSO} + \text{O}_3 \rightarrow \text{DS} + 2\text{O}_2) = (3.0 \pm 1.0) \times 10^{-14} \text{ cm}^3 \text{ molecule}^{-1} \text{ s}^{-1}$ both at 300 K. The application of our results to the oxidation mechanism of H₂S in the atmosphere is discussed.

Introduction

The HS and HSO radicals are of interest because they play important roles in the H₂S oxidation processes that may contribute to the production of atmospheric H₂SO₄. HS is known to be the product of the well-characterized reaction of H₂S and OH.^{1,2} The subsequent oxidation of HS by NO₂³⁻⁵ or O₃⁵⁻⁷ leads to HSO production. There are two published reports of the rate constant for reaction 1. Friedl et al.⁸ measured $k_1 = (3.2 \pm 1.0) \times 10^{-12}$



cm³ molecule⁻¹ s⁻¹ at 298 K using a discharge flow reactor with laser-induced fluorescence HS detection. They attributed an observed HS regeneration to the reaction HSO + O₃ \rightarrow HS + 2O₂, for which they inferred a rate constant of $(1.0 \pm 0.4) \times 10^{-13} \text{ cm}^3 \text{ molecule}^{-1} \text{ s}^{-1}$. A discharge flow-mass spectrometry study of reaction 1 by Schönle et al.⁵ gave $k_1 = (2.9 \pm 0.6) \times 10^{-12} \text{ cm}^3 \text{ molecule}^{-1} \text{ s}^{-1}$, but no HS regeneration was reported. They observed HSO as the product of reaction 1. No direct measurements have been reported for reaction 2.



Other possibly important oxidation processes for HS and HSO in the atmosphere include their reactions with O₂ and NO₂. All previous work failed to observe a reaction between O₂ and HS^{3,8-11} or HSO.¹² But even with the lowest reported limits for these two

(1) Sze, N. D.; Ko, M. K. W. *Atmos. Environ.* **1980**, *14*, 1223.

(2) Leu, M. T.; Smith, R. J. *J. Phys. Chem.* **1982**, *86*, 73.

(3) Wang, N. S.; Lovejoy, E. R.; Howard, C. J. *J. Phys. Chem.* **1987**, *91*, 5743.

(4) Bulatov, V. P.; Kozliner, M. Z.; Sarkisov, O. M. *Khim. Fiz.* **1984**, *3*, 1300.

(5) Schönle, G.; Rahman, M. M.; Schindler, R. N. *Ber. Bunsen-Ges. Phys. Chem.* **1987**, *91*, 66. Several rate coefficients reported by Schönle et al. were recently revised: Schindler, R. N.; Benter, T. *Ibid.* **1988**, *92*, 588. The data quoted in the present work are the revised values.

(6) Schurath, U.; Weber, M.; Becker, K. H. *J. Chem. Phys.* **1977**, *67*, 110.

(7) Kendall, D. J. W.; O'Brien, J. J. A.; Sloan, J. J. *Chem. Phys. Lett.* **1984**, *110*, 183.

(8) Friedl, R. R.; Brune, W. H.; Anderson, J. G. *J. Phys. Chem.* **1985**, *89*, 5505.

(9) Black, G. J. *Chem. Phys.* **1984**, *80*, 1103.

(10) Tsee, J. J.; Wampler, F. B.; Oldenborg, R. C.; Rice, W. W. *Chem. Phys. Lett.* **1981**, *82*, 80.

(11) Stachnik, R. A.; Molina, M. J. *J. Phys. Chem.* **1987**, *91*, 4603.

* Author to whom correspondence should be addressed at NOAA, R/E/AL2, 325 Broadway, Boulder, CO 80303.

reaction rate constants, O_2 is still a potentially important oxidant for HS and HSO because of its high concentration in air. NO_2 reacts very rapidly with HS, $k(HS + NO_2) = 6.7 \times 10^{-11} \text{ cm}^3 \text{ molecule}^{-1} \text{ s}^{-1}$ from our measurement,³ while other workers have reported rate constants in the range $(2.4\text{--}8.6) \times 10^{-11} \text{ cm}^3 \text{ molecule}^{-1} \text{ s}^{-1}$ at room temperature. HSO radicals also react with NO_2 very rapidly. Three groups reported reaction rate constants of 4×10^{-12} ,⁴ $(6.5 \pm 0.6) \times 10^{-12}$,⁵ and $(9.6 \pm 2.4) \times 10^{-12} \text{ cm}^3 \text{ molecule}^{-1} \text{ s}^{-1}$ at room temperature. This reaction is thus the only established path for HSO oxidation. Nevertheless, NO_2 may not be an important oxidant for HS and HSO under some conditions due to its highly variable concentration in the atmosphere. Thus, O_2 and O_3 are potentially important HS and HSO atmospheric oxidants.

In this paper, which is a continuation of our previous studies of H_2S oxidation,^{3,12} we report results on reactions 1 and 2 and discuss their atmospheric relevance.

Experimental Section

The discharge flow laser magnetic resonance (LMR) system used in this study has been described in detail^{3,13} and will not be discussed here. The LMR spectrometer offers sensitive detection not only to HS (detection limit (DL) = 1×10^9 molecules cm^{-3}) and HSO (DL = 5.5×10^9 molecules cm^{-3}) but also to OH (DL = 6×10^7 molecules cm^{-3}) and HO_2 (DL = 4×10^8 molecules cm^{-3}).¹² This provides the ability to identify some reaction products and to study the reaction mechanism.

The HS radicals were produced via reaction 3; $k_3 = 1.2 \times 10^{-12} \text{ cm}^3 \text{ molecule}^{-1} \text{ s}^{-1}$.¹⁴ The H atoms were produced from a 1%



H_2 in He mixture in a microwave discharge and were reacted with the ethylene sulfide, C_2H_4S , in a fixed sidearm reactor or a movable inlet. Reaction 3 was used as the HS source in our earlier study of the $HS + NO_2$ reaction.³ We demonstrated that C_2H_4S does not contribute to HS regeneration and does not participate in secondary reactions, although it does react rapidly with OH. The latter reaction, $k \approx 6 \times 10^{-11} \text{ cm}^3 \text{ molecule}^{-1} \text{ s}^{-1}$, effectively scavenges OH. When the DS reactant was used, a D_2 in He mixture was used to produce atomic D for the analogous reaction, $D + C_2H_4S \rightarrow DS + C_2H_4$.

Although the fast reaction



$k_4 = 1.5 \times 10^{-10} \text{ cm}^3 \text{ molecule}^{-1} \text{ s}^{-1}$,¹⁵ worked well in our previous studies,^{3,12} it was not used in the present study for the reaction rate constants measurements because of complications from a reaction between H_2S and O_3 , as will be discussed.

Reaction 1 was used to produce HSO radicals in a sidearm reactor under conditions such that the reaction went to >99.7% completion. The concentration of O_3 in the source reactor was about 3×10^{14} molecules cm^{-3} and was about 4×10^{13} molecules cm^{-3} upon dilution in the flow tube.

Calibrations of $[HSO]$ relative to $[HS]$ were made using reactions 1 and 5; $k_5 = 6.7 \times 10^{-11} \text{ cm}^3 \text{ molecule}^{-1} \text{ s}^{-1}$.³



Ozone was stored on silica gel at 196 K and was eluted from the trap with a measured flow of He, F_{He} . The O_3 partial pressure, P_{O_3} , was measured by passing the O_3 -He mixture through a 3- or a 10-cm-length absorption cell. The absorption cross section of O_3 at $\lambda = 254 \text{ nm}$ was taken as $1.15 \times 10^{-17} \text{ cm}^2$.¹⁶ The O_3 flow rate, F_{O_3} , was calculated from F_{He} , P_{O_3} , and the total pressure in the absorption cell, P_A , $F_{O_3} = F_{He}P_{O_3}/(P_A - P_{O_3})$.

The He (>99.9996%, analyzed) carrier gas was passed through a molecular sieve filled trap cooled in liquid N_2 . CF_4 (>99.9%),

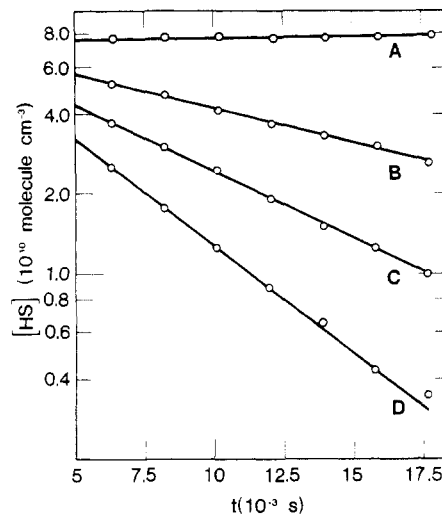


Figure 1. HS decay plots, $T = 297 \text{ K}$, $P = 1.0 \text{ Torr}$, $v = 2600 \text{ cm s}^{-1}$. $[O_3] = 0$ (A); 1.27 (B); 2.54 (C); 4.28 (D); all in $10^{13} \text{ molecules cm}^{-3}$ units.

H_2S (>99.999%), and H_2 (>99.999%) were diluted in He and used without purification. Ethylene sulfide (Aldrich, 99%) was degassed at -77 C . NO_2 was synthesized by reacting purified NO with an excess of O_2 (>99.97%) at a pressure of about 900 Torr and was stored as a liquid in a stainless steel cylinder. The NO_2 was flowed into the flow tube reactor with the cylinder immersed in an ice-cooled bath. The gas flow meters and pressure transducers were calibrated as before.³

Results

All the kinetic measurements were made under pseudo-first-order conditions with $[O_3]$ in large excess over the radical $[R]$, where $R = HS, DS, \text{ or } HSO$. The initial radical concentrations, $[R]_0$, were kept low to avoid possible interferences from radical-radical reactions and to ensure pseudo-first-order kinetics, $[HS]_0$ and $[DS]_0 \leq 1 \times 10^{11}$, $[HSO]_0 \leq 2 \times 10^{11}$ molecules cm^{-3} with $[O_3] \approx (30\text{--}4,000)[R]_0$. The rate equation is expressed as

$$-v \frac{d(\ln [R])}{dz} = k[O_3] = k^1 \quad (6)$$

where v is the average flow velocity in the flow tube (cm s^{-1}), z is the reaction distance (cm) measured from the tip of the movable inlet to the detection zone, k^1 is the first-order rate constant (s^{-1}) determined from the slope of a plot of $\ln [R]$ vs z , and k is the second-order rate constant.

HS + O_3 Reaction. The rate constant for reaction 1 was measured in pressures of 1–2.2 Torr of He at temperatures between 296 and 431 K. A fixed sidearm reactor was used for HS generation via reaction 3. At 296 K a source reactor attached to the movable inlet was also used for some measurements. No reaction rate constants for reaction 1 were measured at $T < 296 \text{ K}$ because the HS radical loss on the flow tube wall was too large. The flow velocity was between 970 and 3050 cm s^{-1} , and z was varied by about 30 cm. Figure 1 shows a set of typical HS decay plots. The decay data labeled A at the top of the figure indicates the HS concentration with no O_3 added. Its slope gives the first-order HS loss on the wall of the movable inlet. Each k^1 was corrected for the HS loss on the movable inlet ($\leq 15 \text{ s}^{-1}$) and axial diffusion ($\leq 3\%$) as described before.³ Curved HS decay plots were observed when high $[O_3]$ and slow flow velocities were used. These data were fitted by computer simulations to evaluate reaction 2, as will be discussed.

The k^1 vs $[O_3]$ plot for the 297 K data is shown in Figure 2 and gives a second-order rate constant $k_1 = (4.39 \pm 0.11) \times 10^{-12} \text{ cm}^3 \text{ molecule}^{-1} \text{ s}^{-1}$ as the slope of the line. The uncertainty represents 2 standard deviations of the slope from the linear least-squares fit. The experimental conditions and the k_1 measurements are summarized in Table I.

The estimated accuracy of the rate constant measurements is derived from error estimates for gas flow rates ($\pm 3\%$), temperature

(12) Lovejoy, E. R.; Wang, N. S.; Howard, C. J. *J. Phys. Chem.* **1987**, *91*, 5749.

(13) Stimpfle, R. M.; Perry, R. A.; Howard, C. J. *J. Chem. Phys.* **1979**, *71*, 5183.

(14) Lee, J. H.; Stief, L. J. *J. Chem. Phys.* **1977**, *67*, 1705.

(15) Agrawalla, B. S.; Setser, D. W. *J. Phys. Chem.* **1986**, *90*, 2450.

(16) DeMore, W. B.; Raper, O. J. *J. Phys. Chem.* **1964**, *68*, 412.

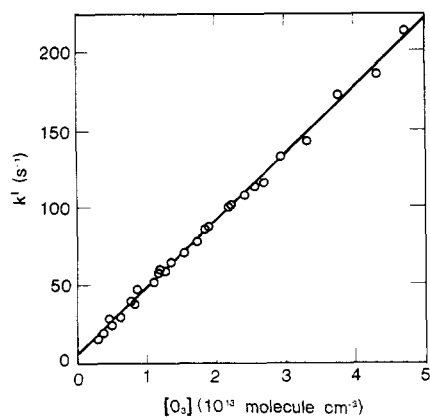


Figure 2. Plot of k^1 vs $[O_3]$ data at 297 K for reaction 1. The k^1 values have been corrected for wall loss and axial diffusion as described in ref 3.

TABLE I: Summary of Our HS + O₃ Reaction Data

T, K	no. of expts	P, Torr	ν range, cm s ⁻¹	[O ₃], 10 ¹³ molecules cm ⁻³	k^1 , 10 ⁻¹² cm ³ molecule ⁻¹ s ⁻¹
296 ^b	9	1.1	2190	0.85–3.72	4.56 ± 0.91
297	27	1.0–2.2	970–2600	0.30–4.68	4.39 ± 0.88
336	10	1.0–2.0	1485–3035	0.47–2.80	4.88 ± 0.98
377	18	1.1–1.2	2235–2820	0.26–2.80	5.51 ± 1.10
431	18	1.1–1.2	1515–2455	0.23–2.83	5.95 ± 1.19

^a Error limits represent the estimated accuracy at 95% confidence level. ^b Data taken with HS source attached to the movable inlet. All other data were taken with the fixed sidearm source.

(±1%), pressure (±1%), O₃ concentration (±8%), flow tube radius (±1%), and the slope of the decay plot (±5%), which gives a total error of about ±10% at the 95% confidence level. This can be compared to the uncertainties derived from fits to the k^1 vs $[O_3]$ plots, which are between 2.4 and 12%. Combining the estimated error with a factor for possible systematic errors yields a value of about 20% at the 95% confidence level for the overall uncertainty in the value of k_1 at each temperature.

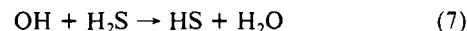
When the HS reactant was prepared via the F + H₂S reaction, curved decay plots were observed and lower k_1 values were obtained. The value of k_1 was found to decrease systematically with increasing [H₂S]. At 298 K and 1.03 Torr with [H₂S] = 2.0 × 10¹² molecules cm⁻³ in the flow tube, k_1 = 3.94 × 10⁻¹² cm³ molecule⁻¹ s⁻¹ was measured. This k_1 value is about 11% smaller than that obtained by using the C₂H₄S source. In a measurement at 1.47 Torr and 298 K the [H₂S] was intentionally kept high: [H₂S] = 7.5 × 10¹³ molecules cm⁻³ in the flow tube. Three first-order HS decay rate constants were measured as the function of [O₃]: k^1 = 26 s⁻¹ at [O₃] = 1.1 × 10¹³ molecules cm⁻³, k^1 = 48 s⁻¹ at [O₃] = 2.0 × 10¹³ molecules cm⁻³, and k^1 = 55 s⁻¹ at [O₃] = 2.9 × 10¹³ molecules cm⁻³. The k_1 values calculated from these data are 2.36 × 10⁻¹², 2.40 × 10⁻¹², and 1.90 × 10⁻¹² cm³ molecule⁻¹ s⁻¹, respectively. They are 45–57% lower than the k_1 results obtained with the C₂H₄S source. Similar results were obtained in nine other sets of measurements at temperatures ranging from 263 to 358 K using the F + H₂S source. In every case the k_1 value derived was lower than the corresponding result obtained with the H + C₂H₄S source reaction. The deviations ranged from about 10% to about 60% lower. The fact that the F + H₂S source gave results that varied with the [H₂S] and [O₃] and curved decay plots, whereas the H + C₂H₄S source did not, led us to concentrate on the F + H₂S + O₃ system as the cause of the discrepancy. The H + C₂H₄S source did give curved decay plots at high [O₃] and long reaction time, but this observation was attributed to HS regeneration via the HSO + O₃ reaction as will be discussed.

Four different possible problems with the F + H₂S source were considered and evaluated: (1) radical generation by the reaction of H₂S with O₃, (2) HS regeneration by the reaction of H₂S with OH, which is formed by secondary chemistry, (3) HS formation

by a reaction sequence initiated by the reaction of O₃ with CF_x ($x = 1, 2, \text{ or } 3$) radicals from the CF₄/He discharge used for the F atom source, and (4) O₃ loss in the reactor due to reaction with the H₂S.

Black⁹ reported observing spontaneous HS production when H₂S and O₃ were mixed. We observed no HS production when H₂S and O₃ were mixed in our reactor, but it should be noted that the concentrations were much smaller by a factor of about 100 in our experiments.

Regarding the second consideration, as discussed below, OH radicals were detected in our HS/O₃ reaction mixture, although Friedl et al.⁸ did not observe OH. The OH can regenerate HS via reaction 7, where $k_7 = 4.7 \times 10^{-12}$ cm³ molecule⁻¹ s⁻¹.¹⁷ This

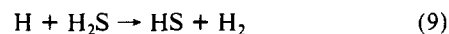


would cause decay plot curvature of the type observed and result in a low value of k_1 . To test for this possibility a large concentration of OH scavenger, C₂F₃Cl, was added to suppress HS regeneration:



where $k_8 = 6 \times 10^{-12}$ cm³ molecule⁻¹ s⁻¹ in 1 Torr of He at 296 K.¹⁸ From several measurements we found the scavenger had no effect, for example, with [C₂F₃Cl] = 2 × 10¹⁴ molecules cm⁻³, which gives $k^1(OH + C_2F_3Cl) = 1200$ s⁻¹ and with [H₂S] = 8.2 × 10¹² molecules cm⁻³, a $k_1 = 2.92 \times 10^{-12}$ cm³ molecule⁻¹ s⁻¹ was measured. This showed that reaction 7 played a negligible role in the systematic irregularities when a high [H₂S] was used.

Next we considered the F atom source, a microwave discharge in CF₄, as a possible cause for the observed variation in k_1 . The concern was that CF_x radicals from the discharge tube might initiate secondary chain reactions that could generate HS radicals or destroy O₃ in the flow tube reactor. Another HS source reaction employing H₂S was used to evaluate possible interferences from CF_x radicals:



where $k_9 = 7 \times 10^{-13}$ cm³ molecule⁻¹ s⁻¹.¹⁹ The H atoms were produced by a microwave discharge in a 1% H₂ in He mixture. The [H₂S] was high to complete the slow reaction 9. At 298 K and 1.42 Torr with [H₂S] = 9.1 × 10¹³ molecules cm⁻³, the k_1 calculated from the HS decay plots ranged from 4.0 × 10⁻¹² to 2.3 × 10⁻¹² cm³ molecule⁻¹ s⁻¹ at [O₃] = (0.82–3.77) × 10¹³ molecules cm⁻³. Thus the results obtained by using both F + H₂S and H + H₂S as HS source reactions were consistent, indicating that complications from CF_x-initiated chain reactions were not the reason for the strange results.

From the above test results, it seemed that H₂S itself must be involved in the observed irregularities in the study of reaction 1. Indeed previous work by Schönle et al.⁵ and Black⁹ reported evidence of a reaction between H₂S and O₃. To test the fourth consideration, a study of reaction 1 was made with the H + C₂H₄S source and with H₂S added to the flow tube with carrier gas. The measured first-order HS loss systematically decreased when H₂S was present in the flow tube. For example, the first-order HS loss changed from 150 s⁻¹, when [H₂S] = 0, to 137 s⁻¹, when [H₂S] = 2.2 × 10¹³ molecules cm⁻³, at [O₃] = 3.61 × 10¹³ molecules cm⁻³ in the flow tube, P = 1.1 Torr, and T = 296 K. Although the effect of excess H₂S was quantitatively smaller in the test experiments with the C₂H₄S source reaction, it was evident that H₂S does effect a variation in k_1 . It is possible that the presence of C₂H₄S in some way inhibits the effect of H₂S on the k_1 measured.

A qualitative evaluation of the reaction between H₂S and O₃ was made to investigate its possible interference in the HS/O₃

(17) DeMore, W. B.; Molina, M. J.; Sander, S. P.; Golden, D. M.; Hampson, R. F.; Kurylo, M. J.; Howard, C. J.; Ravishankara, A. R. NASA Panel for Data Evaluation; *Chemical Kinetics and Photochemical Data for Use in Stratospheric Modeling*; JPL Publication 87-41; Jet Propulsion Laboratory: Pasadena, CA, 1987.

(18) Howard, C. J. *J. Chem. Phys.* **1976**, *65*, 4771.

(19) Kurylo, M. J.; Peterson, N. C.; Braun, W. *J. Chem. Phys.* **1971**, *54*, 943.

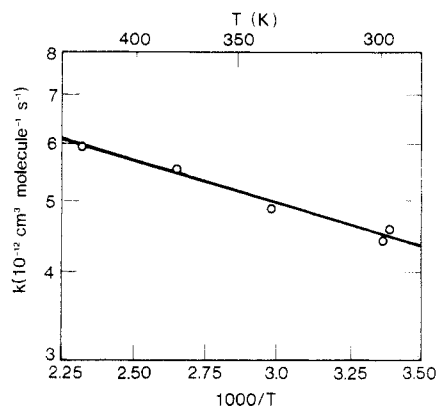


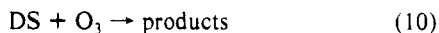
Figure 3. Arrhenius plot of HS + O₃ reaction data. The line indicates $k(T) = (1.1 \pm 0.2) \times 10^{-11} \exp[-(280 \pm 50)/T] \text{ cm}^3 \text{ molecule}^{-1} \text{ s}^{-1}$ obtained from a linear least-squares fit.

system. Two absorption cells for [O₃] measurement were connected in series by a ~50-cm-long 1/4-in.-o.d. Teflon tube. The [O₃] was measured in an O₃-He mixture that was passed through both cells. A gas inlet located approximately in the middle of the Teflon tube admitted an H₂S-He mixture. The H₂S and O₃ streams are allowed to mix before they passed through the downstream absorption cell. The O₃ loss upon the H₂S addition can be measured by this configuration. About 11% of O₃ was destroyed by H₂S when [O₃] $\approx 3.3 \times 10^{15}$ molecules cm⁻³, [H₂S] $\approx 2.2 \times 10^{15}$ molecules cm⁻³, and the reaction time was ~0.1 s in the Teflon tube. An ozone loss was obtained consistently in other similar experiments. In general the amount of ozone lost was much smaller than required to quantitatively explain our kinetics results and was not reproducible from time to time. We believe that the reaction takes place on the surface of the tube as will be discussed.

Our observations regarding the source reactions are summarized as follows: (1) The H + C₂H₄S source gave consistent, well-behaved, and reproducible results. These were the only results we used to evaluate k_1 . (2) The F + H₂S source at low concentrations of H₂S and O₃ gave results that were consistent with the H + C₂H₄S source. But this source in general gave results that included curved decay plots, lower values of k_1 , and variations in the value of k_1 , which depended upon the H₂S and O₃ concentrations.

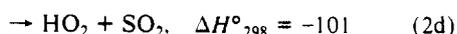
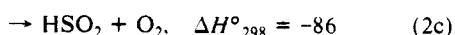
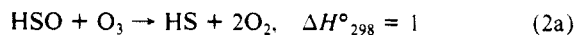
A least-squares fit of our data on reaction 1 to the Arrhenius equation, as shown in Figure 3, gives $k_1(T) = (1.13 \pm 0.08) \times 10^{-11} \exp(-276 \pm 23)/T \text{ cm}^3 \text{ molecule}^{-1} \text{ s}^{-1}$, where the error limits are the standard deviations of the coefficients determined from the fit. Our recommended expression is $k_1(T) = (1.1 \pm 0.2) \times 10^{-11} \exp(-280 \pm 50)/T \text{ cm}^3 \text{ molecule}^{-1} \text{ s}^{-1}$. As discussed above the estimated error limits for our measurements are $\pm 20\%$. If the data are extrapolated beyond the temperature range of our measurements, the uncertainty will be larger.

DS + O₃ Reaction. Twelve k^1 measurements were made on reaction 10 at 1.1 Torr and 300 K to investigate the possibility



of an isotope effect in reaction 1. The [O₃] was in the range $(0.28\text{--}5.3) \times 10^{13}$ molecules cm⁻³. A rate constant of $(4.0 \pm 0.8) \times 10^{-12} \text{ cm}^3 \text{ molecule}^{-1} \text{ s}^{-1}$ was determined from the slope of the k^1 vs [O₃] plot.

H₂O + O₃ Kinetics. The following are some of the possible reaction channels for reaction 2 (ΔH°_{298} in kcal mol⁻¹):



The reaction enthalpies are calculated by using $\Delta H_f^\circ_{298}$ values

TABLE II: Results of Computer Simulations and Measured k_{2a}

<i>T</i> , K	k_1 , ^a 10 ⁻¹² cm ³ molecule ⁻¹ s ⁻¹	k_{11} , ^b s ⁻¹	k_{12} , ^c s ⁻¹	k_{2a} , ^d 10 ⁻¹⁴ cm ³ molecule ⁻¹ s ⁻¹
297	4.4	19-9	10-5	7.0 ± 3.0
377	5.4	40-10	20-5	9.0 ± 3.0
405	5.7	40-10	25-5	10 ± 4

^a The k_1 was from our measurements and was fixed. ^b k_{11} was also from direct measurements. ^c k_{12} was measured in ref 12 and the present study. The input data for k_{11} and k_{12} were varied to analyze the sensitivities of the fits. ^d k_{2a} is the preferred value based on the simulations.

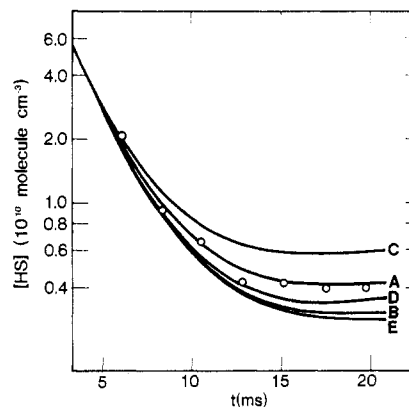
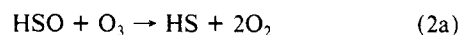
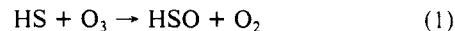


Figure 4. Simulations of reaction 2a at 297 K and 1 Torr. Fixed parameters: [O₃] = 9.3×10^{13} molecules cm⁻³ and $k(\text{HS} + \text{O}_3) = 4.4 \times 10^{-12} \text{ cm}^3 \text{ molecule}^{-1} \text{ s}^{-1}$. The experimental data are shown as points (O), and the curves represent calculated fits with k_{2a} (in cm³ molecule⁻¹ s⁻¹) = 5×10^{-14} (B, D, E), 7×10^{-14} (A), and 1×10^{-13} (C). $k_{11} = 9 \text{ s}^{-1}$ in A-C and 19 s^{-1} in D. $k_{12} = 5 \text{ s}^{-1}$ in A-D and 10 s^{-1} in E.

from Baulch et al.²⁰ and Lovejoy et al.¹². The direct measurement of k_{2a} is difficult in our system because the much faster subsequent reaction HS + O₃ regenerates HSO radicals. However, a measurement was possible by fitting the experimental HS decay with data generated by using a Fortran computer model based on the GEAR differential equation algorithm. A description of this computer program was given by Hills and Howard.²¹ The program was used to compute HS profiles to fit those measured in the experiments. The calculated HS profiles were most sensitive to the input k_{2a} when the [HS] plots were curved, so the experimental data were taken at high [O₃] or long reaction time, when the curved [HS] plots were observed. Four reactions were employed in the simulations:



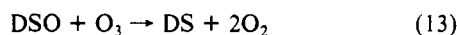
Reaction 11 corresponds to the HS loss on the flow tube wall. The HSO loss, reaction 12, incorporated wall reaction and reactions 2a (=2b-e), which was a small ($k_{2a}[\text{O}_3] \leq 15 \text{ s}^{-1}$) first-order process at constant [O₃]. An independent measurement of k_{2a} is given below. Table II lists the rate parameters used in the simulations and the preferred k_{2a} obtained at three different temperatures. For the model, k_1 was taken from our measurements. The wall loss for HS, k_{11} , was also obtained from direct measurements. The values of k_{12} were measured in the study of Lovejoy et al.¹² and the present study. Because a reduction in the wall loss rates for HS and HSO was observed after the wall was exposed to O₃, the values of k_{11} and k_{12} were varied to examine

(20) Baulch, D. L.; Cox, R. A.; Hampson, R. F.; Kerr, J. A.; Troe, J.; Watson, R. T. Evaluation Kinetic and Photochemical Data For Atmospheric Chemistry: Supplement II CODATA Task Group on Gas Phase Chemical Kinetics. *J. Phys. Chem. Ref. Data* **1984**, *13*, 1259.

(21) Hills, A. J.; Howard, C. J. *J. Chem. Phys.* **1984**, *81*, 4458.

the sensitivity of the results to these parameters. The variable parameter in these model fits was k_{2a} . Figure 4 shows five fits to one set of experimental data taken at 297 K. The value of k_{2a} was varied from 5×10^{-14} (curves B, D, and E) to 7×10^{-14} (curve A) and 1×10^{-13} (curve C) $\text{cm}^3 \text{molecule}^{-1} \text{s}^{-1}$. It was found that the output HS profiles from the model were not very sensitive to the parameters k_{11} and k_{12} . When k_{11} was changed from 9 (curve B) to 19 s^{-1} (curve D), the initial slopes for HS decay plots remained unchanged and the [HS] varied less than 17%. When k_{12} was varied from 5 (curve B) to 10 s^{-1} (curve E), the changes in [HS] were less than 7%. While k_{2a} was doubled from 5×10^{-14} (curve B) to $1 \times 10^{-13} \text{ cm}^3 \text{molecule}^{-1} \text{s}^{-1}$ (curve C), a significant change ($\sim 100\%$) was found in [HS] at a reaction time of ~ 20 ms. A preferred value of k_{2a} of $7 \times 10^{-14} \text{ cm}^3 \text{molecule}^{-1} \text{s}^{-1}$ at 297 K was obtained on the basis of the best fits in the simulations. Table II also lists preferred values for k_{2a} at 377 and 405 K. Here the uncertainties are large because of the uncertainties in the model parameters such as the absolute reaction time and the radical wall loss rates in the presence of O₃. Our scant data on k_{2a} can be used to estimate the Arrhenius expression $k_{2a}(T) = 2.7 \times 10^{-13} \exp[-400/T]$; here the uncertainties in the parameters are quite large.

An analysis of the DS + O₃ reaction data gives a rate constant of $(4 \pm 2) \times 10^{-14} \text{ cm}^3 \text{molecule}^{-1} \text{s}^{-1}$ for reaction 13 at 300 K; DSO was not detectable in our experiments.



The products of the HS + O₃ reaction mixture were measured to obtain information about the product channels. Four radical species, HS, HSO, OH, and HO₂, were measured by the LMR spectrometer in the HS/O₃ reaction mixture. Here HS radicals were produced in the reactor attached to the movable inlet by the F + H₂S reaction instead of the H + C₂H₄S reaction, so that any OH product would not be removed by the fast reaction OH + C₂H₄S ($k \approx 6 \times 10^{-11} \text{ cm}^3 \text{molecule}^{-1} \text{s}^{-1}$).³ The [H₂S] was kept low, $= 3.3 \times 10^{12} \text{ molecules cm}^{-3}$, in the flow tube to suppress HS regeneration via the OH + H₂S reaction. HSO was found to be the major primary product on the basis of its appearance simultaneous with the loss of HS. The amount of HSO formed was compared to that from the analogous reaction 5 between HS and NO₂, for which we believe HSO to be the only significant product.³ Small amounts of OH and HO₂ also were formed. Some OH and HO₂ were most likely produced by the subsequent reaction 2 and some was probably produced by impurities, likely H from the source reactor. The HSO₂ product from reaction 2 is measurable, after it has been converted to HO₂ by reaction with O₂:



where $k_{14} = 3 \times 10^{-13} \text{ cm}^3 \text{molecule}^{-1} \text{s}^{-1}$.¹²

The following are typical results of a product analysis study carried out at low conversion to minimize secondary reactions. At $T = 297 \text{ K}$, $P = 1.3 \text{ Torr}$, a reaction time of 35 ms, $[\text{HS}]_0 = 1.2 \times 10^{11} \text{ molecules cm}^{-3}$, and $[\text{O}_3] = 5.1 \times 10^{13} \text{ molecules cm}^{-3}$, HSO was found to be the primary product with a concentration of $6.2 \times 10^{10} \text{ molecules cm}^{-3}$. The [OH] and [HO₂] were observed to be low, at about 1.5×10^{10} and $0.3 \times 10^{10} \text{ molecules cm}^{-3}$, respectively. No significant changes of [HS] and [HSO] were measured in the presence of $8.3 \times 10^{14} \text{ molecules cm}^{-3}$ of O₂, but [OH] and [HO₂] increased by about 23% and 40%. The increase in [HO₂] could be attributed to reaction 14. But the reason for the observed [OH] increase is not obvious. The reaction 2 mechanism shows that some HO_x (H, OH, or HO₂) is formed by the HSO + O₃ reaction through channels 2b–e. A quantitative evaluation of the branching ratios of reaction 2 from the product analysis was difficult because of the poor reproducibility, especially in [OH] and [HO₂], of these measurements. The production of some HO_x species in the source reactor may have contributed to this problem.

The reaction rate constant k_{2a} ($k_{2a} = k_{2b} + k_{2c} + k_{2d} + k_{2e}$) was directly measured. Since HS is not regenerated through reactions 2b–e, the rate constant k_{2a} was derived from the observed

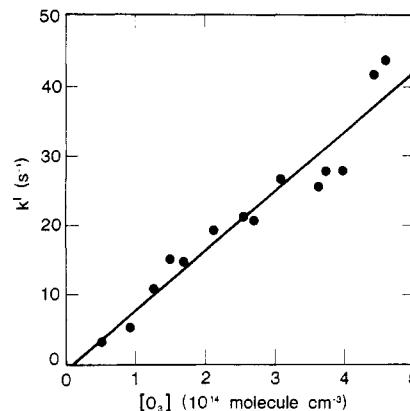


Figure 5. k^1 vs $[\text{O}_3]$ plot for reaction 2a, $\text{HSO} + \text{O}_3 \rightarrow \text{products}$, at 404 K.

TABLE III: Summary of Results on HSO and DSO Reactions with O₃

T, K	k , $10^{-14} \text{ cm}^3 \text{molecule}^{-1} \text{s}^{-1}$
A. $\text{HSO} + \text{O}_3 \rightarrow \text{HS} + 2\text{O}_2^a$ (k_{2a})	
297	7 ± 3
377	9 ± 3
405	10 ± 4
B. $\text{HSO} + \text{O}_3 \rightarrow \text{Products}^b$ (k_{2a})	
296	3.5 ± 1.5
404	8.6 ± 3.5
C. $\text{DSO} + \text{O}_3 \rightarrow \text{DS} + 2\text{O}_2^a$ (k_{13a})	
300	4 ± 2

^a Rate constants derived from computer model fits to HS or DS decay data as discussed in text. ^b $k_{2a} = k_{2b} + k_{2c} + k_{2d} + k_{2e}$, directly measured as described in text.

TABLE IV: Comparison of HS + O₃ Reaction Rate Constant Measurements at Room Temperature

T, K	P, Torr	method ^a	k_1 , $10^{-12} \text{ cm}^3 \text{molecule}^{-1} \text{s}^{-1}$	ref
297	1–2.2	DF-LMR	4.39 ± 0.88	this work ^b
298	1.9	DF-MS	2.9 ± 0.6	Schönle et al. ⁵
298	2–8	DF-LIF	3.2 ± 1.0	Friedl et al. ⁸

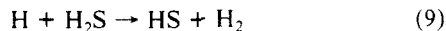
^a DF = discharge flow; LMR = laser magnetic resonance; MS = mass spectrometry; LIF = laser-induced fluorescence. ^b $k(T) = (1.1 \pm 0.2) \times 10^{-11} \exp[(-280 \pm 50)/T] \text{ cm}^3 \text{molecule}^{-1} \text{s}^{-1}$, for $296 \text{ K} \leq T \leq 431 \text{ K}$.

loss of HSO in the presence of O₃. The H + C₂H₄S reaction was used as the HS source, and HSO was generated in the sidearm reactor via reaction 1. With O₃ reactant added through the movable inlet, the HSO disappearance as a function of reaction distance gave the first-order HSO loss. Measurements were made at 296 and 404 K. The [O₃] ranged from 0.5×10^{14} to $9.3 \times 10^{14} \text{ molecules cm}^{-3}$, the flow velocities were between 750 and 1150 cm s^{-1} , and the pressures were 1.4–2.2 Torr. The k^1 vs [O₃] plot for data taken at 404 K is shown in Figure 5. Table III summarizes the kinetics results of reactions 2 and 13. The error limits include a factor for the estimated systematic error and the precision at the 95% confidence level. Table III summarizes the kinetic results of reactions 2 and 13. A crude estimate of the Arrhenius parameters from our data at two temperatures gives $k_{2a}(T) = 1 \times 10^{-12} \exp[-1000/T] \text{ cm}^3 \text{molecule}^{-1} \text{s}^{-1}$, where the uncertainties on the parameters are very large.

Discussion

Table IV summarizes all of the known studies of the HS + O₃ reaction kinetics. Two previous studies of reaction 1 employed H₂S in the HS source. Schönle et al.⁵ used the F + H₂S reaction to generate HS radicals. The [H₂S] was relatively low in their system: $[\text{H}_2\text{S}] = (2-3) \times 10^{12} \text{ molecule cm}^{-3}$. They reported $k_1 = (2.9 \pm 0.6) \times 10^{-12} \text{ cm}^3 \text{molecule}^{-1} \text{s}^{-1}$, which is in good agreement with the value obtained by Friedl et al.,⁸ (3.2 ± 1.0)

$\times 10^{-12}$ cm³ molecule⁻¹ s⁻¹. The H₂S concentration in the work of Friedl et al. was relatively high, [H₂S] $\geq 5 \times 10^{13}$ molecules cm⁻³, because they employed a slower HS source reaction:



where $k_9 = 7 \times 10^{-13}$ cm³ molecule⁻¹ s⁻¹.¹⁹ They observed curved HS decay plots, and their k_1 was derived from the initial slopes of their decay plots. Some curved decay plots were also observed in our study, but Schönle et al. did not report any curvature. The k_1 value measured at room temperature in our study agrees with that reported by Friedl et al.⁸ within the combined error limits but does not overlap with that from Schönle et al.⁵ Complications from OH chain reactions or CF_x radicals from the source have been proven not to be important to this systematic error.

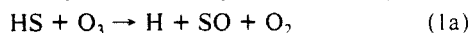
In an unsuccessful attempt to study reaction 1, Black⁹ observed HS production and O₃ destruction due to a reaction between H₂S and O₃. Other workers^{22,23} have also reported a reaction between H₂S and O₃. The possibility of a systematic error associated with the use of H₂S as an HS precursor has been investigated in the present study. We attributed the discrepancies between the results from the C₂H₄S and H₂S sources to a wall reaction between H₂S and O₃. This surface reaction may be enhanced by the presence of elemental sulfur, which we believe is present from our F + H₂S source. Schönle et al.⁵ studied reaction 15 by observing H₂S loss



in the presence of O₃. Some loss was observed, but it did not obey simple kinetics laws. They derived an upper limit for the reaction rate constant (assumed second-order) of $k_{15} < 10^{-14}$ cm³ molecule⁻¹ s⁻¹ for their reactor. Earlier Becker et al.²⁴ studied reaction 15 in a 220-m³ spherical reactor at low pressure (<0.1 Torr) and reported $k_{15} \leq 2 \times 10^{-20}$ cm³ molecule⁻¹ s⁻¹. We believe that the reaction takes place on the wall of the reactors and that the much lower value of k_{15} measured by Becker et al. can be accounted for by the small surface area to volume ratio of their reactor.

Some of the HSO produced in reaction 1 has been observed to be electronically excited HSO*(\tilde{A}^2A').^{6,7} However the participation of HSO* in the chemical reactions is very unlikely as pointed out by Friedl et al.⁸ because its radiative lifetime is very short, ~ 100 μ s,²⁵ which implies a first-order radiative decay rate constant of 10^4 s⁻¹. Typical first-order reactive losses for HS and HSO in the present study are < 250 s⁻¹.

The observation of emission from electronically excited HSO was the basis for an early determination of the heat of formation of the radical by Schurath et al.⁶ Their measured short-wavelength limit of emission at about 520 nm was taken as the total exothermicity of the HS + O₃ reaction, which leads to a value of $\Delta H_f^\circ(\text{HSO}) \approx 14$ kcal mol⁻¹. More recent work by Davidson et al.,²⁶ as discussed by Friedl et al.⁸ and Lovejoy et al.,¹² establishes a lower value, $\Delta H_f^\circ(\text{HSO}) \approx -1.4$ kcal mol⁻¹. Although it was not discussed in previous studies of the HS + O₃ reaction kinetics, the reaction is sufficiently exothermic to produce atomic hydrogen:



where $\Delta H_f^\circ \approx -14.5$ kcal mol⁻¹. This channel may account for some of the OH and HO₂ radicals we observe, since the H is rapidly converted to OH and HO₂ in the presence of O₃. As noted by Kawasaki et al.²⁵ the short-wavelength extinction of HSO emission observed by Schurath et al. corresponds to the H-SO dissociation limit. From our product studies we estimate that channel 1a accounts for $\leq 15\%$ of the HS + O₃ reaction products and HSO + O₂ accounts for the balance, $\geq 85\%$. The formation of H + SO probably occurs through decomposition of an energetic HSO* intermediate.

(22) Glavas, S.; Toby, S. *J. Phys. Chem.* **1975**, *79*, 779.

(23) Gliński, R. J.; Sedarski, J. A.; Dixon, D. A. *J. Am. Chem. Soc.* **1982**, *104*, 1126.

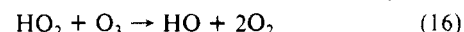
(24) Becker, K. H.; Inocencio, M. A.; Schurath, U. *Int. J. Chem. Kinet. Symp.* **1975**, *1*, 205.

(25) Kawasaki, M.; Kasatani, K.; Tanahashi, S.; Sato, H.; Fujimura, Y. *J. Chem. Phys.* **1983**, *78*, 7146.

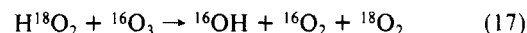
(26) Davidson, F. E.; Clemo, A. R.; Duncan, G. L.; Browett, R. J.; Hobson, J. H.; Grice, R. *Mol. Phys.* **1982**, *46*, 33.

We know of no previous report of the temperature dependence of reaction 1. A normal Arrhenius behavior with an activation energy of 0.55 kcal mol⁻¹ for reaction 1 was obtained in the present study. Unlike the radical-radical reaction HS + NO₂, which has a negative temperature dependence and which probably proceeds via an addition mechanism,³ reaction 1 probably occurs via a direct abstraction mechanism. This contention agrees with the conclusion of Kendall et al.,⁷ who stated that no long-lived HS-O₃ intermediate is formed in reaction 1 from their observation of a non-Boltzmann energy distribution in the HSO* product. Friedl et al.⁸ used activated complex theory to calculate a value for the A factor of 3×10^{-12} cm³ molecule⁻¹ s⁻¹ for an open-chain HS-O₃ complex. The A factor reported in the present study, 1.2×10^{-11} cm³ molecule⁻¹ s⁻¹, is 4 times larger, which means that the transition state is slightly looser than the one used in their calculation.

Although our k_{2a} value at 297 K, $(7.0 \pm 3.0) \times 10^{-14}$ cm³ molecule⁻¹ s⁻¹, is 30% lower than the value of Friedl et al.,⁸ $(1.0 \pm 0.4) \times 10^{-13}$ cm³ molecule⁻¹ s⁻¹, the two values overlap within the combined error limits. Friedl et al. reported that reaction 2a was the only product channel for reaction 2 based on the lack of OH production and the absence of a kinetic isotope effect. For the DSO + O₃ reaction, they obtained $k_{13a} = 9 \times 10^{-14}$ cm³ molecule⁻¹ s⁻¹, which is 2.2 times larger than our value. They made an analogy between reaction 2 and reaction 16, whereby the O



atom is transferred to O₃ by HSO to give HS + 2O₂. It has recently been shown that this is not the predominant mechanism in the HO₂ + O₃ reaction. In a study using isotope-labeled HO₂ (reaction 17), Sinha et al.²⁷ found ¹⁶OH to be the major product



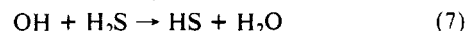
(75 \pm 10%), indicating that the H-¹⁸O₂ bond is broken. This result does not support the analogy between reactions 2 and 16, although it is interesting to note that our crude Arrhenius expression for $k_{2a}(T)$ has characteristics similar to those of the HO₂ + O₃ reaction, namely, a small A coefficient and a low E_a .

If reaction 2a were the only channel for reaction 2, we should not observe HSO loss upon addition of O₃, since the subsequent reaction 1 regenerates HSO immediately. We did observe a net loss of HSO and measured the rate coefficient, $k_{2a} = 3.5 \times 10^{-14}$ cm³ molecule⁻¹ s⁻¹ at 296 K. Also some of the OH and HO₂ radicals detected as products in our HS/O₃ were most likely derived from reaction 2, indicating the existence of channels other than reaction 2a in reaction 2. Our study showed that the HS-O bond-breaking channel, reaction 2a, predominates over the other product routes, reaction 2 α . This supports the original discovery of the reaction by Friedl et al.⁸

Atmospheric Implications

It is believed that the oxidation of reduced sulfur compounds is a major natural source of SO₂ (or SO₄²⁻) in the environment. Recent estimates of the global emission of reduced sulfur compounds into the atmosphere range from 65 to 125 Tg(S) year⁻¹ (Tg(S) = 10¹² g of sulfur).²⁸ This is comparable to the anthropogenic sulfur emission (SO₂), which is estimated at about 70–100 Tg(S) year⁻¹.²⁸ The H₂S emission originates mainly from soils, plants, coastal waters, and volcanoes and is estimated to be 5–8 Tg(S) year⁻¹. Thus it may account for a significant part of the total natural sulfur emission.

Figure 6 is a schematic of the H₂S atmospheric oxidation mechanism following what we believe are the dominant steps. The oxidation process is initiated by the well-established reaction



The lifetime of H₂S due to oxidation by OH in the troposphere

(27) Sinha, A.; Lovejoy, E. R.; Howard, C. J. *J. Chem. Phys.* **1987**, *87*, 2122.

(28) Andreae, M. O. In *The Biogeochemical Cycling of Sulfur and Nitrogen in the Remote Atmosphere*; Galloway, J. N., Charlson, R. J., Andreae, M. O., Eds.; Reidel: Dordrecht, 1985; pp 5–25.

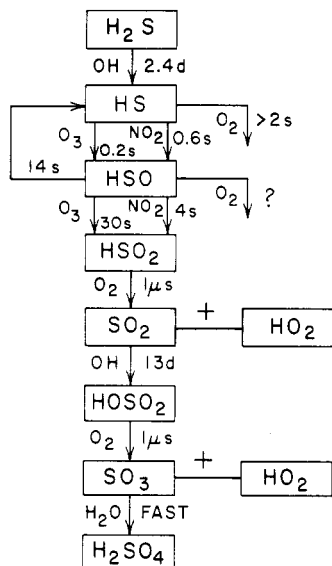


Figure 6. H₂S oxidation mechanism in air. Schematic shows the major known steps in the mechanism for the atmospheric oxidation of H₂S. The reactants and reaction lifetimes are indicated next to the arrows. The lifetimes are estimated by using the room-temperature rate coefficient and typical atmospheric concentrations of the reactants: [OH] = 1 × 10⁶, [O₃] = 1 × 10¹², [NO₂] = 2.5 × 10¹⁰, and [O₂] = 5 × 10¹⁸ all in molecule cm⁻³ units.

is estimated to be about 2.4 days²⁹ by using the recommended value of $k_7 = 4.7 \times 10^{-12} \text{ cm}^3 \text{ molecule}^{-1} \text{ s}^{-1}$ ¹⁷ at 298 K with a diurnally averaged OH concentration of 1 × 10⁶ molecules cm⁻³.³⁰

The major oxidants of atmospheric radicals are NO₂, O₃, and O₂. The mole fraction of NO₂ in the troposphere ranges from ~10 ppb (ppb = parts per billion) in polluted air to ~10 ppt (ppt = parts per trillion) in areas remote from sources.³¹ The atmospheric O₃ mole fraction is less variable than that of NO₂ and is reported as ~40 ppb by Fehsenfeld et al.³² HS produced in reaction 7 is subsequently oxidized by O₃ very rapidly:



with a short lifetime, ~0.2 s. NO₂ also reacts with HS very rapidly and produces HSO:

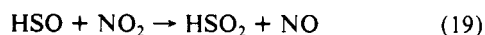


But this reaction is less important than reaction 1 in clean air due to the low mole fraction of NO₂ (<1 ppb).³¹ The HS radicals also may be oxidized by O₂ to give OH and SO:



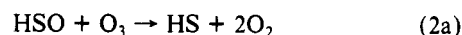
Although no reaction has been observed, the lowest limit on k_{18} ($\leq 4 \times 10^{-19} \text{ cm}^3 \text{ molecule}^{-1} \text{ s}^{-1}$) reported by Stachnik and Molina¹¹ still allows for a significant amount of reaction due to the high concentration of O₂ in air ($\approx 5 \times 10^{18} \text{ molecules cm}^{-3}$).

On the basis of the work of Lovejoy et al.¹² and the present study, the oxidation of HSO in the atmosphere is accomplished mainly by NO₂ and O₃:

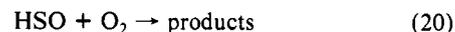


HSO has a lifetime of ~4 s in the troposphere due to its reaction

with NO₂, when NO₂ is present at the 1 ppb level. Reaction 2a



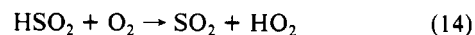
regenerates HS radicals, so it does not contribute to the HSO oxidation but recycles HSO to the reduced form. However, O₃ oxidizes HSO via reaction 2α, which may produce SO, HSO₂, or SO₂. Reaction 2α is less important than reaction 19 when the [NO₂] is significant, ≥0.1 ppb. Our previous study of reaction 20 failed to observe any evidence of a reaction,¹² $k_{20} \leq 2 \times 10^{-17}$



cm³ molecule⁻¹ s⁻¹, but it remains potentially important in the atmosphere due to the high concentration of O₂ and requires further study before a definitive statement can be made on the kinetics of HSO.

Since the HSO + O₃ reaction to give HSO₂ + O₂ is highly exothermic, $\approx 86 \text{ kcal mol}^{-1}$, the HSO₂ product is likely to possess a great deal of internal energy. Thus channel 2e may represent the unimolecular decomposition of a hot HSO₂ product. Alternatively, in channel 2d the departing O₂ fragment carries off the labile H, which seems less likely than either reaction 2c or 2e. Atmospheric pressure may deactivate or stabilize excited products and thus alter the product ratios. In any case, the final products of channels 2b–e are probably OH or HO₂ and SO₂ under atmospheric conditions.

The HSO₂ produced in reaction 19 and probably reaction 2α and the SO produced in reaction 2α are rapidly oxidized to SO₂ by O₂:

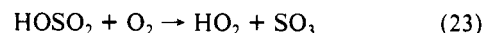


where $k_{14} = 3 \times 10^{-13} \text{ cm}^3 \text{ molecule}^{-1} \text{ s}^{-1}$ ¹² and $k_{21} = 8.4 \times 10^{-17} \text{ cm}^3 \text{ molecule}^{-1} \text{ s}^{-1}$ at 298 K.¹⁷ The HSO₂ molecule has a very short lifetime (~1 μs) in the air due to reaction with O₂.

We conclude that SO₂ is a key intermediate in the H₂S oxidation process. A major sink for SO₂ in the atmosphere is its aqueous oxidation to SO₄²⁻. It has been estimated by Hegg³³ that this removal process is at least as important as the gas-phase termolecular reaction



where $k_{22} = 8.8 \times 10^{-13} \text{ cm}^3 \text{ molecule}^{-1} \text{ s}^{-1}$ is the effective bimolecular rate constant for reaction 22 in 1 atm of air at 300 K.¹⁷ Reaction 22 is generally accepted as the main atmospheric gas-phase oxidation reaction of SO₂.^{34–36} It is a slow process with a lifetime for SO₂ of ~2 weeks because of the low atmospheric [OH]. The HOSO₂ has a very short lifetime of ~1 μs due to the subsequent oxidation by O₂:



where $k_{23} = (4.4 \pm 0.7) \times 10^{-13} \text{ cm}^3 \text{ molecule}^{-1} \text{ s}^{-1}$.³⁷ Sulfuric acid is thereafter formed rapidly by the addition of H₂O to SO₃,³⁸ which takes place either in the gas phase or on the surface of droplets or particles:



The OH radicals are involved in both of the rate-determining steps, reactions 7 and 22, of the atmospheric H₂S oxidation process. Interestingly there is no net loss of HO_x due to the production

(29) The lifetimes of sulfur compounds are calculated by using the room-temperature reaction rate constants.

(30) Prinn, R.; Cunnold, D.; Rasmussen, R.; Simmonds, P.; Alyea, F.; Crawford, A.; Fraser, P.; Rosen, R. *Science* **1987**, *238*, 945. They reported a globally averaged tropospheric [OH] = $(7.7 \pm 1.4) \times 10^5 \text{ molecules cm}^{-3}$.

(31) Logan, J. A. *J. Geophys. Res.* **1983**, *88*, 10785.

(32) Fehsenfeld, F. C.; Bollinger, M. J.; Liu, S. C.; Parrish, D. D.; McFarland, M.; Trainer, M.; Kley, D.; Murphy, P. C.; Albritton, D. L. *J. Atmos. Chem.* **1983**, *1*, 87.

(33) Hegg, D. A. *J. Geophys. Res.* **1985**, *90*, 3773.

(34) Calvert, J. G.; Lazrus, A. L.; Kok, G. L.; Hiekes, B. G.; Walega, J. G.; Lind, J.; Cantrell, C. A. *Nature (London)* **1985**, *317*, 27.

(35) *Acid Deposition: Atmospheric Processes in Eastern North America*; National Research Council, National Academy Press: Washington, DC, 1983.

(36) Benson, S. W. *Chem. Rev.* **1978**, *78*, 23.

(37) Gleason, J. F.; Sinha, A.; Howard, C. J. *J. Phys. Chem.* **1987**, *91*, 719.

(38) (a) Castleman, A. W. Jr.; Davis, R. E.; Munkelwitz, H. R.; Tang, I. N.; Wood, W. P. *Int. J. Chem. Kinet. Symp.* **1975**, *1*, 629. (b) Wang, X.; Jin, Y. G.; Suto, M.; Lee, L. C.; O'Neal, H. E. *J. Chem. Phys.* **1988**, *89*, 4853.

of HO₂ radicals in reactions 14 and 23. The overall homogeneous gas-phase production of H₂SO₄ takes on the order of 2-3 weeks. This means that the acid may be deposited some distance from the H₂S source as the gas is transported in an air mass. Although some uncertainties remain, especially concerning the products of the HSO reactions, a general picture has been formed for the overall atmospheric H₂S oxidation process.

Acknowledgment. This work was supported by NOAA as part of the National Acid Precipitation Assessment Program. We thank our colleague Dr. A. R. Ravishankara for helpful comments on this paper.

Registry No. HS, 13940-21-1; HSO, 62470-71-7; O₃, 10028-15-6; D₂, 7782-39-0.

Kinetics of Diffusion-Influenced Reactions Studied by Brownian Dynamics

Huan-Xiang Zhou

Laboratory of Chemical Physics, National Institute of Diabetes and Digestive and Kidney Diseases, National Institutes of Health, Bethesda, Maryland 20892 (Received: February 22, 1990; In Final Form: May 30, 1990)

An algorithm is developed for calculating the time-dependent rate coefficient $k(t)$ of diffusion-influenced reactions. This algorithm exploits the well-known relationship between the pair distribution function of the reactants, which defines $k(t)$, and the survival probability, which can be easily simulated by using Brownian dynamics. Various boundary conditions are discussed. The efficiency of the algorithm is assessed. For several cases where $k(t)$ is analytically known, this algorithm produces results that are in excellent agreement with their analytical counterparts over the entire time range. For other cases, the implementation of the algorithm does not depend on the particular geometry or interaction potential.

I. Introduction

The kinetics of diffusion-influenced reactions, characterized by the time-dependent rate coefficient $k(t)$, is analytically solvable for a limited number of cases.¹⁻¹² The rate coefficient $k(t)$ is directly related to observed quantities in experiments such as ligand binding to macromolecules,¹³ fluorescence quenching,^{11,14} and the self-assembly of multisubunit proteins. In this paper, we present a computational algorithm for calculating $k(t)$ based on Brownian dynamics simulations.

The problem under consideration can be formulated as follows. We are interested in the diffusion-influenced reaction between two species, A and B. The concentration, $C(\mathbf{r})$, of species B at \mathbf{r} relative to species A normalized by $C(\infty)$ is defined as the pair distribution function, $p(\mathbf{r}, t)$, between the two species. The pair distribution function $p(\mathbf{r}, t)$ is assumed to satisfy the Smoluchowski equation^{1,10,11a}

$$\partial p(\mathbf{r}, t) / \partial t = -\nabla \cdot \mathbf{J}(\mathbf{r}, t) \equiv \nabla \cdot D e^{-\beta U(\mathbf{r})} \nabla e^{\beta U(\mathbf{r})} p(\mathbf{r}, t) \quad (1.1)$$

where $\beta = (k_B T)^{-1}$, D is the relative diffusion coefficient of A and B (i.e., $D = D_A + D_B$), and $U(\mathbf{r})$ is the potential of mean force between A and B. Up to time $t = 0$, A and B are inert and B

has an equilibrium (i.e., Boltzmann) distribution around A

$$p(\mathbf{r}, 0) = e^{-\beta U(\mathbf{r})} \quad (1.2)$$

At $t = 0$, A and B are turned into reactive species (e.g., by photolysis). This is characterized by a radiation boundary condition²

$$-\mathbf{n} \cdot \mathbf{J}(\mathbf{r}, t) \equiv \mathbf{n} \cdot D e^{-\beta U(\mathbf{r})} \nabla e^{\beta U(\mathbf{r})} p(\mathbf{r}, t) = \kappa(\mathbf{r}) p(\mathbf{r}, t), \quad \mathbf{r} \in \Gamma \quad (1.3a)$$

where Γ is the boundary between A and B, \mathbf{n} is the normal of Γ , and $\kappa(\mathbf{r})$ is the space-dependence intrinsic bimolecular rate constant. Usually, part of Γ is reflecting; this is described by $\kappa(\mathbf{r}) = 0$. The absorbing extreme is described by $\kappa(\mathbf{r}) = \infty$. The outer boundary condition is given by

$$p(\infty, t) = 1 \quad (1.3b)$$

The quantity of interest is the time-dependent rate coefficient defined by the equation

$$k(t) = - \int_{\Gamma} dS \mathbf{n} \cdot \mathbf{J}(\mathbf{r}, t) \quad (1.4)$$

The reason that $k(t)$ of eq 1.4 has the character of a rate coefficient is that the total concentrations of A, $A(t)$, satisfies the kinetic equation^{10,11a}

$$dA(t)/dt = -k(t) C(\infty) A(t) \quad (1.5)$$

in which it is assumed that B is in excess so that the change of $C(\infty)$ with time is negligible.

In principle, one can solve eq 1.1 for $p(\mathbf{r}, t)$ subject to the initial condition 1.2 and the boundary conditions 1.3 and integrate (eq 1.4) to obtain $k(t)$. This becomes formidable when the geometry or potential gets complicated. The purpose of this paper is to find an algorithm for calculating $k(t)$ when arbitrary geometry and potential are present.

In essence, our algorithm exploits the well-known relationship between the pair distribution function $p(\mathbf{r}, t)$ and the survival probability $S(t|\mathbf{r}_0)$ ^{15,16}

$$p(\mathbf{r}_0, t) = e^{-\beta U(\mathbf{r}_0)} S(t|\mathbf{r}_0) \quad (1.6)$$

Technically, $S(t|\mathbf{r}_0)$ is the probability that reactants started (at time $t = 0$) at \mathbf{r}_0 will survive (i.e., not react) at time t . From the

- (1) Smoluchowski, M. Z. *Phys. Chem.* **1917**, *92*, 129.
- (2) Collins, F. C.; Kimball, G. E. *J. Colloid Sci.* **1949**, *4*, 425.
- (3) Weller, A. Z. *Phys. Chem.* **1957**, *79*, 551.
- (4) Carslaw, H. S.; Jaeger, J. C. *Conduction of Heat in Solids*, 2nd ed.; Oxford University Press: New York, 1959.
- (5) Hong, K. M.; Noolandi, J. *J. Chem. Phys.* **1978**, *68*, 5163, 5172.
- (6) Rice, S. A.; Butler, P. R.; Pilling, M. J.; Baird, J. K. *J. Chem. Phys.* **1979**, *70*, 4001.
- (7) (a) Pedersen, J. B. *J. Chem. Phys.* **1980**, *72*, 3904. (b) Pedersen, J. B.; Sibani, P. *Ibid.* **1981**, *75*, 5368. (c) Sibani, P.; Pedersen, J. B. *Phys. Rev. Lett.* **1983**, *51*, 148.
- (8) Flannery, M. R. *Phys. Rev.* **1982**, *A25*, 3403.
- (9) (a) Shoup, D.; Szabo, A. *J. Electroanal. Chem.* **1982**, *140*, 237. (b) Szabo, A.; Shoup, D.; Northrup, S. H.; McCammon, J. A. *J. Chem. Phys.* **1982**, *77*, 4484.
- (10) Rice, S. A. Diffusion-Limited Reactions. In Bamford, C. H.; Tipper, C. F. H.; Compton, R. G., Eds. *Comprehensive Chemical Kinetics*; Elsevier: Amsterdam, 1985; Vol. 25.
- (11) (a) Szabo, A. *J. Phys. Chem.* **1989**, *93*, 6929. (b) Agmon, N.; Szabo, A. *J. Chem. Phys.* **1990**, *92*, 5270.
- (12) Traytak, S. D. *Chem. Phys.* **1990**, *140*, 281.
- (13) The binding of carbon monoxide to protoheme provides an outstanding example.
- (14) Zhou, H. X.; Szabo, A. *J. Chem. Phys.* **1990**, *92*, 3874.

(15) Onsager, L. *Phys. Rev.* **1938**, *54*, 554.

(16) Tachiya, M. *J. Chem. Phys.* **1978**, *69*, 2375.